Effects of coherent ferroelastic domain walls on the thermal conductivity and Kapitza conductance in bismuth ferrite

Patrick E. Hopkins, Carolina Adamo, Linghan Ye, Bryan D. Huey, Stephen R. Lee et al.

Related Articles

Additional information on Appl. Phys. Lett.

Effects of coherent ferroelastic domain walls on the thermal conductivity and Kapitza conductance in bismuth ferrite

Patrick E. Hopkins,[1,a] Carolina Adamo,[2] Linghan Ye,[3] Bryan D. Huey,[3] Stephen R. Lee,[4] Darrell G. Schlom,[2] and Jon F. Ihlefeld[4,b]

[1]*Department of Mechanical and Aerospace Engineering, University of Virginia, Charlottesville, Virginia 22904, USA*
[2]*Department of Materials Science and Engineering, Cornell University, Ithaca, New York 14853, USA*
[3]*Institute of Materials Science, University of Connecticut, Storrs, Connecticut 06269, USA*
[4]*Sandia National Laboratories, Albuquerque, New Mexico 87123, USA*

Ferroelectric and ferroelastic domain structure has a profound effect on the piezoelectric, ferroelectric, and dielectric responses of ferroelectric materials. However, domain walls and strain field effects on thermal properties are unknown. We measured the thermal conductance from 100–400 K of epitaxially grown $BiFeO_3$ thin films with different domain variants, each separated primarily by 71° domain walls. We determined the Kapitza conductance across the domain walls, which is driven by the strain field induced by the domain variants. This domain wall Kapitza conductance is lower than the Kapitza conductance associated with grain boundaries in all previously measured materials. © 2013 American Institute of Physics. [http://dx.doi.org/10.1063/1.4798497]

Ferroelectric and ferroelastic domain structure has a profound effect on the piezoelectric, ferroelectric, and dielectric responses of ferroelectric materials. These responses drive the development of capacitors, non-volatile memory, sensors, and tunnel junctions.[1–3] Recently, progress in thin film growth of materials utilizing these ferroelectric effects has given rise to the promise of novel device applications on the nanoscale.[4,5] Much of this recent interest has been based on bismuth ferrite ($BiFeO_3$), a rhombohedrally distorted perovskite exhibiting room temperature coexistence of ferroelectric and antiferromagnetic orders, yielding many unusual properties.[6,7]

Several recent studies have shown that through the use of a vicinal substrates, it is possible to engineer the domain structure of epitaxial $BiFeO_3$ films.[8–11] This is accomplished on $SrTiO_3$ single-crystalline substrates by utilizing symmetry breaking step edges resulting from intentional miscuts along high-symmetry crystallographic directions. For example, through the use of a sufficient miscut along the [100] direction of a (001)-oriented $SrTiO_3$ substrate, the 1.4% smaller lattice parameter of the $SrTiO_3$ (3.905 Å) compared to $BiFeO_3$ (3.96 Å) results in a compressive strain in the $(010)_p$ and $(001)_p$ planes at the step edge and forces the polarization axes to be parallel to $[111]_p$ or $[\bar{1}11]_p$. This results in a film with only two possible domain variants with polar axes parallel to these directions. A sufficient miscut along the $\langle 110 \rangle$ substrate direction constrains the film in the $(100)_p$, $(010)_p$, and $(001)_p$ planes and confines the polar axis to be parallel to $[111]_p$ and results in a film with just one domain variant and no ferroelastic domain walls. In the absence of step edges, compressive stain exists on only the $(001)_p$ plane and the polarization axis has equal probability of being parallel to $[111]_p$, $[\bar{1}11]_p$, $[1\bar{1}1]_p$, or $[\bar{1}\bar{1}1]_p$, and there are four possible domain variants in the film.

Given the growth and substrate dependent domain structures that $BiFeO_3$ exhibits, its properties and responses to various stimuli can be affected by the presence of the various domain walls. These properties must be considered and well characterized as $BiFeO_3$ thin films are considered for use in various nanodevices. Specifically, in this Letter, we report on the thermal transport in $BiFeO_3$ thin films grown on different non-vicinal and vicinal cut substrates to produce the domain variants mentioned above. The domain walls in the $BiFeO_3$ films, which occur on the nanometer scale, cause additional phonon scattering events that will add additional resistances to thermal transport.[12–14] The challenge in utilizing $BiFeO_3$ in future applications, therefore, lies in understanding how phonon transport is affected by domain wall scattering. Although previous work has extensively examined the effects of grain boundaries on phonon transport and thermal conductivity,[15–20] these grain boundaries can represent incoherent, highly disordered regions. The domain walls in $BiFeO_3$, however, are perfectly coherent and are only ~1–2 nm in thickness.[21,22]

To study the effects of domain variants on thermal properties, we measure the thermal conductance of a series of $BiFeO_3$ thin films with different domain variants. Piezo force microscopy (PFM) reveals a corresponding variation in the average domain wall density, based on polarization mapping that allows domain wall identification, local polarization rotation, and interfacial charging to be determined with 4.5 nm resolution. We measure the thermal conductance of the $BiFeO_3$ films with time domain thermoreflectance (TDTR)[23] from 100–400 K. The effective thermal conductivities that we observe in the $BiFeO_3$ films vary based on the density of domain walls in the thin film, where the presence of more domains leads to a decrease in thermal conductivity. We relate the measured conductances to the thermal boundary conductance across the $BiFeO_3$ domain walls. The thermal boundary conductances across the coherent domain walls are lower than the thermal boundary conductances

a)Electronic mail: phopkins@virginia.edu
b)Electronic mail: jihlefe@sandia.gov

associated with grain boundaries in silicon, strontium titanate, and yttria-stabilized zirconia (YSZ).

We used substrate vicinality to prepare a set of epitaxial BiFeO$_3$ films with varying numbers of domain variants and domain wall densities. Films were prepared using adsorption-controlled reactive molecular-beam epitaxy (MBE) on (001)-oriented non-vicinal (oriented within $\pm 0.5°$ of (001)), and vicinal 4° miscut along [100], and vicinal 4° miscut along [110] SrTiO$_3$ substrates. Synthesis details can be found elsewhere.[24,25] All films were phase-pure by X-ray diffraction and were of high crystalline quality with omega rocking curve full width at half maximum values equivalent to the underlying substrates (typically 0.01°).

Figure 1 presents domain orientation maps of the 4-domain (a) and 2-domain (b) variant specimens, deduced from the PFM images (Fig. 1 in supporting information).[40] In almost every case, the domains share the same normal orientation, but the domain density and morphology is distinct for the two specimens. As anticipated, there are far more domains, as well as polarization directions, apparent for the 4-domain film. Images from the 1-domain variant samples exhibited no contrast, signifying a uniform, single polarization.

Focusing on the domain walls, the 4-variant case was found to exhibit 19.90 μm of domain boundary per μm^2 of film area, compared with only 13.98 μm per μm^2 of film for the 2-variant specimen and no measured domain walls for the single-variant specimen. Local polarization rotation angles along every domain wall can additionally be mapped, based on simple lookup tables, which consider the adjacent domain orientations.[26] As with our previous work on similar specimens, all domain boundaries exhibited essentially purely 71° rotations. Domain boundary types can similarly be determined and visualized, including charged (head-to-head, tail-to-tail) and neutral (head-to-tail and tail-to-head) interfaces, as shown in Figs. 1(c) and 1(d) for 4-domain and 2-domain films, respectively. The ratio of charged to neutral domain boundaries is 2.02:1 for the 4-domain variant and 1.05:1 for the 2-domain variant.

With this knowledge of the domain boundary statistics within the films, we measured the thermal conductance of the 30 nm thick BiFeO$_3$ films with TDTR.[23] Our assumptions in this analysis are outlined in the supporting information. The effective thermal conductivities of the BiFeO$_3$ films determined from our TDTR measurements are shown in Fig. 2. We observe a clear trend in the effective thermal conductivities of the BiFeO$_3$ and the number of domain variants. An increase in the number of domain variants and, subsequently, density of domain walls in the film leads to a decrease in thermal conductivity. We ascribe this dependency to phonons scattering in the domain boundaries and creating a temperature gradient across the individual domain walls. More domain variants in the BiFeO$_3$ lead to more domain boundaries as shown in Fig. 1 and therefore increased phonon scattering and lower thermal conductivities. We note that the domain boundaries are coherent, unlike grain boundaries, which are typically highly disordered and thereby force phonon scattering through impurity-like mechanisms. Charged domain walls may be important to the thermal response, but additional experiments are necessary to isolate this effect. We also point out that the thermal conductivities of the BiFeO$_3$ films are most likely affected by size effects due to the thin film geometry; that is, phonon scattering at the film boundaries of the BiFeO$_3$ can cause a reduction in the thermal conductivity of the films as compared to a thicker or "bulk" sample.[27–29] However, since all samples are 30 nm, the finite size of the sample has the same effect in
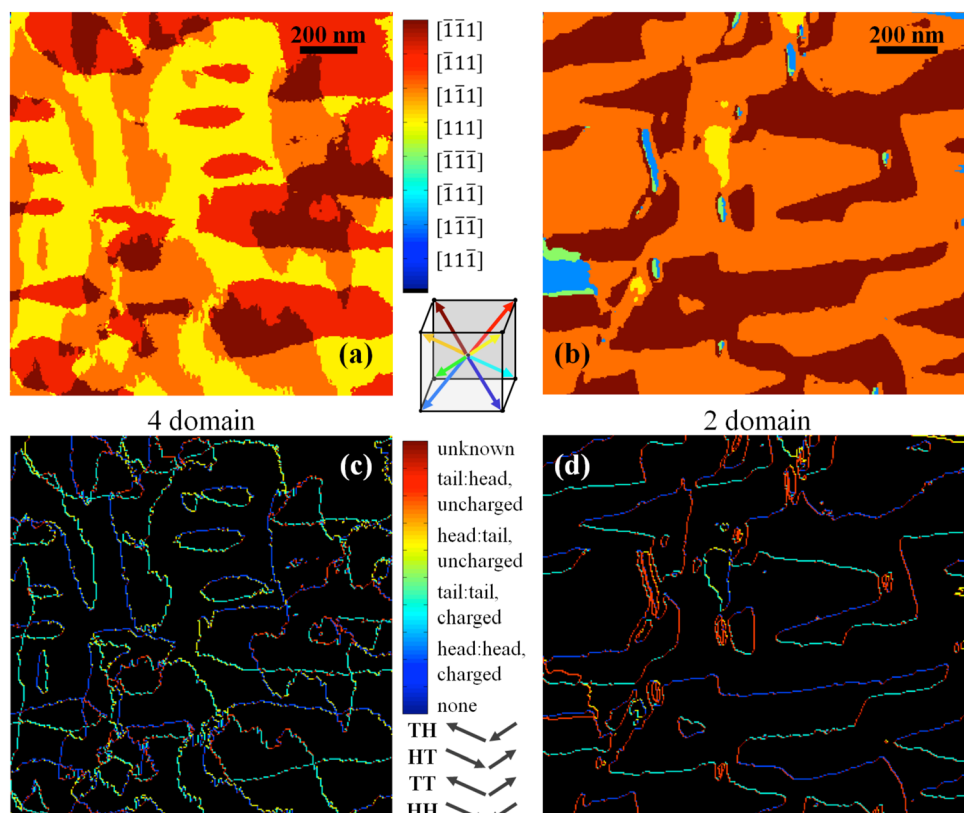

FIG. 1. Ferroelectric domain orientation maps for 4-domain (a) and 2-domain (b) specimens, with corresponding images of domain boundary types and charging in (c) and (d) revealing the substantial difference in domain wall density for distinct polarization variants. The 200 nm scale bars in (a) and (b) apply to all images for each specimen (columns).
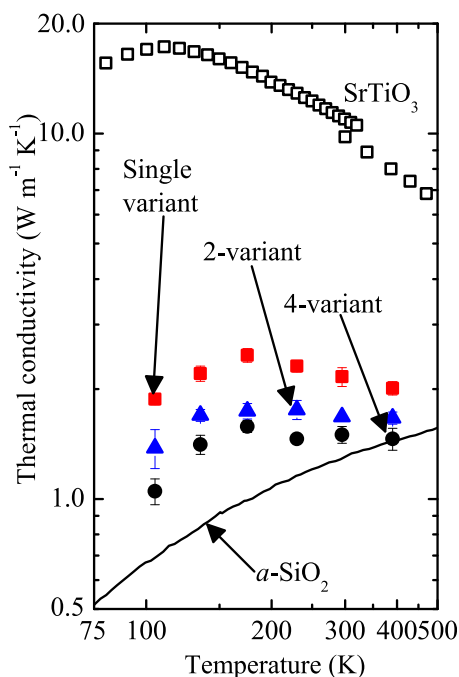
FIG. 2. Effective thermal conductivities of the BiFeO$_3$ films (filled symbols). There is a clear dependence of the thermal transport on the number of domains, which we ascribe to additional temperature drops across the nanometer thick domain walls caused by phonon scattering in the localized strain field. For comparison, we also plot the thermal conductivity of bulk SrTiO$_3$ (open squares, Refs. 20 and 30) and amorphous SiO$_2$ (solid line, Ref. 31).

FIG. 3. Thermal boundary conductance across the domain walls in the BiFeO$_3$ films. For comparison, we also plot the calculated thermal boundary conductance across grain boundaries in YSZ (filled triangles, Ref. 34), silicon (filled circles, Ref. 37), and SrTiO$_3$ (empty triangles, Ref. 20). We also include Si grain boundary thermal boundary conductances determined with molecular dynamics from Refs. 38 and 39. The thermal boundary conductances across the YSZ, Si, and SrTiO$_3$ grain boundaries are consistently higher than the thermal boundary conductances across the BiFeO$_3$ domain boundaries, even though the grain boundaries are highly disordered regions where the domain walls are completely coherent. We also plot the equivalent conductances of some thickness d of SiO$_2$ (solid lines with d indicated in the plot). The thermal boundary conductance across the BiFeO$_3$ domain boundaries is similar to the equivalent conductance of ~10 nm of SiO$_2$.

all of the films, therefore, highlighting the domain wall effects on thermal transport in BiFeO$_3$.

Since the thermal conductivity of BiFeO$_3$ has not been reported elsewhere, we compare these effective thermal conductivities to other material systems to put our reported effective thermal conductivities into perspective. We plot the thermal conductivity of bulk SrTiO$_3$,[20,30] a prototypical perovskite, and amorphous SiO$_2$.[31] The effective thermal conductivities of the BiFeO$_3$ films show temperature dependencies similar to crystalline SrTiO$_3$ (i.e., a slight maximum due to the onset of Umklapp scattering), which is expected since the BiFeO$_3$ films are fully crystalline, but the values are much closer than those of SiO$_2$, especially at elevated temperatures and in the multi-domain samples.

Since the phonon scattering across the domain walls leads to a temperature drop across the domain boundaries, we can quantify the thermal transport across the domain boundaries with a thermal boundary conductance.[32,33] This idea of thermal boundary conductance across domain walls, or "internal interfaces," was first observed in potassium dihydrogen phosphate (KDP) at liquid helium temperatures where phonon transport in the KDP was mostly ballistic, and phonon transmission across the domain walls was nearly entirely specular and elastic.[12,13] To calculate the thermal boundary conductance of the domain walls in the BiFeO$_3$ films, we use a series resistor approach utilizing the data presented in Fig. 2.[34,35] From our domain wall maps, we determine $d = 71.5$ and 50.2 nm for the 2- and 4-domain variant samples, respectively. We calculate the thermal boundary conductance for both the 2- and 4-domain variant cases, and average the resulting values to give the conductance across the coherent domain boundary, shown in Fig. 3. The
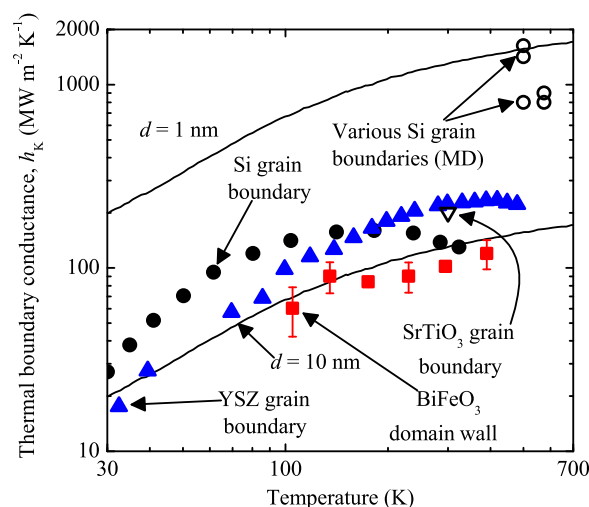
uncertainties in these values are calculated from the standard deviation about of mean values calculated from the 2- and 4-domain variant samples. The domain boundary conductance exhibits values that are similar to typical boundary conductances between well acoustically matched metals and non-metals (i.e., on the order of ~100 MW m^{-2} K^{-1} at room temperature).[36] For comparison, we also plot the thermal boundary conductance across grain boundaries in YSZ,[34] silicon,[37] and SrTiO$_3$.[20] We also include Si grain boundary thermal boundary conductances determined with molecular dynamics (MD) simulations.[38,39] The thermal boundary conductances across the YSZ, Si, and SrTiO$_3$ grain boundaries are consistently higher than the Kapitza conductances across the BiFeO$_3$ domain boundaries, even though the grain boundaries are highly disordered regions, while in contrast, the domain walls are completely coherent. This indicates strongly resistive phonon processes in the domain wall region. To put these values into perspective, we plot the equivalent conductances of some thicknesses, d, of SiO$_2$. These conductances are calculated via $h_{SiO_2} = \kappa_{SiO_2}/d$ where d is indicated in Fig. 3. The thermal boundary conductance across the BiFeO$_3$ domain boundaries are similar to ~10 nm of SiO$_2$, again indicating the relatively high thermal resistivity associated with the domain walls.

The very low thermal boundary conductance across domain boundaries is surprising given the coherency of the interfaces. It is possible that this phenomenon is intrinsic to ferroelastic domain boundaries as Weilert and coworkers measured substantially lower thermal conductivities in polydomain KDP compared to poled crystals.[12,13] Another possible source of the thermal resistance is the presence of inhomogeneous strain at the domain walls. Interestingly,

while PFM was easily able to distinguish the separate domain polarizations in our films, these differing orientations were not identified in high-resolution x-ray diffraction reciprocal space maps as is observed by other researchers (Fig. 4 in the supporting information).[9–11] Instead, in maps collected around the substrate 103 reflection, only single film peaks were observed. For the samples with 4- and 2-domain variants, the film 103_p diffraction peak is accompanied by a broader background, indicative of diffuse scattering. We believe that this diffuse scattering is a direct result of the film thickness being less than the critical thickness for relaxation and a significant amount of inhomogeneous strain being present at the domain boundaries, resulting in this broadening. This is further supported by the apparent lack of the diffuse background in the single domain sample, where no domain boundaries exist and x-ray scattering due to elastic interactions at the boundaries is eliminated. We hypothesize that the potential for significant inhomogeneous strain at the domain boundaries may be a contributing factor to the low thermal boundary conductance across these domain walls. Future studies on the role of film strain certainly are in order to better understand these effects.

In summary, we have investigated the effects of domain variants and domain wall thermal boundary conductance on the thermal transport of $BiFeO_3$ thin films. The effective thermal conductivities that we measured in the $BiFeO_3$ films with TDTR vary based on the domains in the thin film, where more domain walls lead to a decrease in thermal conductivity. At higher temperatures, the effective thermal conductivity of the 4-domain variant $BiFeO_3$ thin films is roughly equivalent to the thermal conductivity of silicon dioxide (SiO_2). We also determine the thermal boundary conductance across the domain walls in our $BiFeO_3$ films. This domain wall thermal boundary conductance is lower than the conductance associated with grain boundaries in previously measured materials, indicating the strong effect domain walls have on phonon scattering and thermal conductance even though domain walls are generally considered to be nearly perfect interfacial regions. Future work in domain wall thermal engineering should focus on studying the influence of domain wall type, domain characteristics (charged or neutral), and population on thermal transport to optimize the performance of practical devices.

[1]K. M. Rabe, J. M. Triscone, and C. H. Ahn, *Physics of Ferroelectrics: A Modern Perspective* (Springer-Verlag, Berlin, 2007).

[2]M. Lines and A. Glass, *Principles and Applications of Ferroelectrics and Related Materials* (Clarendon Press, Oxford, 1979).

[3]J. F. Scott, *Ferroelectric Memories* (Springer-Verlag, Berlin, 2000).

[4]R. Ramesh and N. A. Spaldin, Nature Mater. **6**, 21 (2007).

[5]M. Dawber, K. M. Rabe, and J. F. Scott, Rev. Mod. Phys. **77**, 1083 (2005).

[6]J. Wang, J. B. Neaton, H. Zheng, V. Nagarajan, S. B. Ogale, B. Liu, D. Viehland, V. Vaithyanathan, D. G. Schlom, U. V. Waghmare, N. A. Spaldin, K. M. Rabe, M. Wuttig, and R. Ramesh, Science **299**, 1719 (2003).

[7]R. J. Zeches, M. D. Rossell, J. X. Zhang, A. J. Hatt, Q. He, C.-H. Yang, A. Kumar, C. H. Wang, A. Melville, C. Adamo, G. Sheng, Y.-H. Chu, J. F. Ihlefeld, R. Erni, C. Ederer, V. Gopalan, L. Q. Chen, D. G. Schlom, N. A. Spaldin, L. W. Martin, and R. Ramesh, Science **326**, 977 (2009).

[8]R. R. Das, D. M. Kim, S. H. Baek, C. B. Eom, F. Zavaliche, S. Y. Yang, R. Ramesh, Y. B. Chen, X. Q. Pan, X. Ke, M. S. Rzchowski, and S. K. Streiffer, Appl. Phys. Lett. **88**, 242904 (2006).

[9]Y.-H. Chu, M. P. Cruz, C. H. Yang, L. W. Martin, P.-L. Yang, J. X. Zhang, K. Lee, P. Yu, L. Q. Chen, and R. Ramesh, Adv. Mater. **19**, 2662 (2007).

[10]H. W. Jang, D. Ortiz, S.-H. Baek, C. M. Folkman, R. R. Das, P. Shafer, Y. Chen, C. T. Nelson, X. Pan, R. Ramesh, and C.-B. Eom, Adv. Mater. **21**, 817 (2009).

[11]S. H. Baek, H. W. Jang, C. M. Folkman, Y. L. Li, B. Winchester, J. X. Zhang, Q. He, Y. H. Chu, C. T. Nelson, M. S. Rzchowski, X. Q. Pan, R. Ramesh, L. Q. Chen, and C. B. Eom, Nature Mater. **9**, 309 (2010).

[12]M. A. Weilert, M. E. Msall, A. C. Anderson, and J. P. Wolfe, Phys. Rev. Lett. **71**, 735 (1993).

[13]M. A. Weilert, M. E. Msall, J. P. Wolfe, and A. C. Anderson, Z. Phys. B: Condens. Matter **91**, 179 (1993).

[14]S. Mielcarek, B. Mróz, Z. Tylczyński, P. Piskunowicz, Z. Trybuła, and M. Bromberek, Physica B **299**, 83 (2001).

[15]A. D. McConnell and K. E. Goodson, Ann. Rev. Heat Transfer **14**, 129 (2005).

[16]P. E. Hopkins and L. M. Phinney, J. Heat Transfer **131**, 043201 (2009).

[17]Z. Wang, J. E. Alaniz, W. Jang, J. E. Garay, and C. Dames, Nano Lett. **11**, 2206 (2011).

[18]B. A. Strukov, S. T. Davitadze, S. N. Kravchun, S. A. Taraskin, M. Goltzman, V. V. Lemanov, and S. G. Shulman, J. Phys.: Condens. Matter **15**, 4331 (2003).

[19]S. T. Davitadze, S. N. Kravchun, B. A. Strukov, B. M. Goltzman, V. V. Lemanov, and S. G. Shulman, Appl. Phys. Lett. **80**, 1631 (2002).

[20]Y. Wang, K. Fujinami, R. Zhang, C. Wan, N. Wang, Y. Ba, and K. Koumoto, Appl. Phys. Express **3**, 031101 (2010).

[21]S. Stemmer, S. K. Streiffer, F. Ernst, and M. Ruhle, Philos. Mag. A **71**, 713 (1995).

[22]M. Foeth, A. Sfera, P. Stadelmann, and P. A. Buffat, Jpn. Soc. Electron Microsc. **48**, 717 (1999).

[23]D. G. Cahill, K. E. Goodson, and A. Majumdar, J. Heat Transfer **124**, 223 (2002).

[24]J. F. Ihlefeld, A. Kumar, V. Gopalan, D. G. Schlom, Y. B. Chen, X. Q. Pan, T. Heeg, J. Schubert, X. Ke, P. Schiffer, J. Orenstein, L. W. Martin, Y. H. Chu, and R. Ramesh, Appl. Phys. Lett. **91**, 071922 (2007).

[25]J. F. Ihlefeld, N. J. Podraza, Z. K. Liu, R. C. Rai, X. Xu, T. Heeg, Y. B. Chen, J. Li, R. W. Collins, J. L. Musfeldt, X. Q. Pan, J. Schubert, R. Ramesh, and D. G. Schlom, Appl. Phys. Lett. **92**, 142908 (2008).

[26]J. Desmarais, J. F. Ihlefeld, T. Heeg, J. Schubert, D. G. Schlom, and B. D. Huey, Appl. Phys. Lett. **99**, 162902 (2011).

[27]G. Chen, *Nanoscale Energy Transport and Conversion: A Parallel Treatment of Electrons, Molecules, Phonons, and Photons* (Oxford University Press, New York, 2005).

[28]R. Cheaito, J. C. Duda, T. E. Beechem, K. Hattar, J. F. Ihlefeld, D. L. Medlin, M. A. Rodriguez, M. J. Campion, E. S. Piekos, and P. E. Hopkins, Phys. Rev. Lett. **109**, 195901 (2012).

[29]B. M. Foley, H. J. Brown-Shaklee, J. C. Duda, R. Cheaito, B. J. Gibbons, D. Medlin, J. F. Ihlefeld, and P. E. Hopkins, Appl. Phys. Lett. **101**, 231908 (2012).

[30]C. Yu, M. L. Scullin, M. Huijben, R. Ramesh, and A. Majumdar, Appl. Phys. Lett. **92**, 191911 (2008).

[31]D. G. Cahill, Rev. Sci. Instrum. **61**, 802 (1990).

[32]P. L. Kapitza, Z. Eksp. Teor. Fiz. **11**, 1 (1941).

[33]E. T. Swartz and R. O. Pohl, Rev. Mod. Phys. **61**, 605 (1989).

[34]H. S. Yang, G. R. Bai, L. J. Thompson, and J. A. Eastman, Acta Mater. **50**, 2309 (2002).

[35]C. W. Nan and R. Birringer, Phys. Rev. B **57**, 8264 (1998).

[36]P. M. Norris and P. E. Hopkins, J. Heat Transfer **131**, 043207 (2009).

[37]S. Uma, A. D. McConnell, M. Asheghi, K. Kurabayashi, and K. E. Goodson, Int. J. Thermophys. **22**, 605 (2001).

[38]P. K. Schelling, S. R. Phillpot, and P. Keblinski, J. Appl. Phys. **95**, 6082 (2004).

[39]A. Maiti, G. Mahan, and S. Pantelides, Solid State Commun. **102**, 517 (1997).

[40]See supplementary material at http://dx.doi.org/10.1063/1.4798497 for details of Piezo Force Microscopy characterization of domains, experimental details of TDTR measurements and analysis, and X-ray Diffraction reciprocal space maps.